Transactions of the Materials Research Society of Japan 31[1] 19-22 (2006)

Effect of Sr Substitution for $Ba_2NaNb_5O_{15}$ Thin Films Prepared by Pulsed Laser Deposition

Taro Yamasaki, Tohru Higuchi, Takeshi Hattori and Takeyo Tsukamoto
Department of Applied Physics, Tokyo University of Science, 1-3 Kagurazaka, Shinjuku, Tokyo 162-8601, Japan
Fax: 81-3-5228-8241, e-mail: higuchi@rs.kagu.tus.ac.jp

The Sr-doped $Ba_2NaNb_5O_{15}$ ($Ba_{2-x}Sr_xNaNb_5O_{15}$) thin films were prepared on the $La_{0.05}Sr_{0.95}TiO_3$ substrates by pulsed laser deposition. When the Po_2 and T_{sub} were fixed at 7.5 mTorr and 700°C, respectively, the thin film exhibited a highly *c*-axis orientation and a smooth surface. The *c*-axis orientation and surface roughness do not depend on Sr concentration. These thin films consisted of small grains with diameter of 50~80 nm against the film thickness of 400 nm. The postannelaed $Ba_{2-x}Sr_xNaNb_5O_{15}$ thin films exhibited the good *P-E* hysteresis loops. When the Sr concentration is x=0.7, the remanent polarization (P_r) and coercive field (E_c) were $2P_r$=59.4 μC/cm^2 and $2E_c$=182 kV/cm, respectively.

Key words: $Ba_{2-x}Sr_xNaNb_5O_{15}$, remanent polarization (P_r), $La_{0.05}Sr_{0.95}TiO_3$ substrate, pulsed laser deposition (PLD)

1. INTRODUCTION

Tungsten bronze-type $Ba_2NaNb_5O_{15}$, which belongs to the point group of mm2 at room temperature, is ferroelectric oxide with a tetragonal tungsten bronze-type structure [1-6], as shown in Fig. 1. The $Ba_2NaNb_5O_{15}$ has spontaneous polarization (P_s) of 40 μC/cm^2 and dielectric constant (ε) of 51 parallel to *c*-axis [1-4]. The $Ba_2NaNb_5O_{15}$ has two phase transitions above room temperature [1-4]. One is the ferroelectric phase transition at approximately 560°C, the other is the ferroelastic phase transition at approximately 300°C, which is responsible for the formation of twined substructures. The $Ba_2NaNb_5O_{15}$ bulk crystal has been expected as optical device because the nonlinear optical coefficient is twice as large as that of $LiNbO_3$ [7,8].

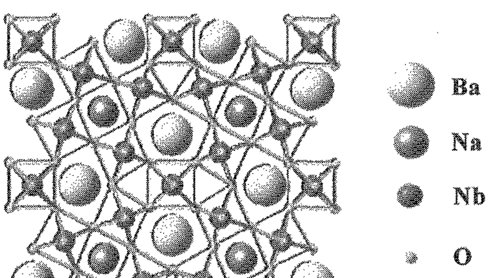

Fig. 1 Crystal structure in the *a-b* plane of $Ba_2NaNb_5O_{15}$.

In recent years, the authors have succeeded in preparation of *c*-axis oriented $Ba_2NaNb_5O_{15}$ thin film on $La_{0.05}Sr_{0.95}TiO_3$ (LSTO) substrate by pulsed laser deposition (PLD) [5-7]. The surface roughness and ferroelectricity depend on oxygen gas pressure (Po_2) and substrate temperature (T_{sub}) during the deposition. When the Po_2 and T_{sub} were fixed at 7.5 mTorr and 700°C, respectively, the thin film exhibited a smooth surface and a relatively good *P-E* hysteresis loop [7]. Its remanent polarization (P_r) and coercive field (E_c) were $2P_r$=48.5 μC/cm^2 and $2E_c$=290 kV/cm, respectively, although the effect of leakage current was induced.

In this study, the $Ba_{2-x}Sr_xNaNb_5O_{15}$ thin films were prepared on LSTO substrates by PLD. The lattice mismatch between $Ba_2NaNb_5O_{15}$ and LSTO was estimated to be approximately 5.2% [7]. In the bulk crystal, the ferroelectric properties, such as Curie temperature (T_c) and ε, can be adjusted by the substitution of Sr^{2+} ion into the Ba^{2+} site [8]. In particular, T_c decreases with increasing Sr concentration, although the P_s does not depend on Sr concentration. However, the ferroelectric and structural properties of $Ba_{2-x}Sr_xNaNb_5O_{15}$ thin films have not been clarified thus far. In this paper, we report the effect of Sr substitution for undoped $Ba_2NaNb_5O_{15}$ thin film.

2. EXPERIMENTAL

$Ba_{2-x}Sr_xNaNb_5O_{15}$ thin films were deposited on (100)-oriented LSTO substrate by PLD method using ceramic target. The single crystals of LSTO substrates, which were grown by the Czochralski method, were obtained from Earth Jewelry Co. Ltd. The $Ba_{2-x}Sr_xNaNb_5O_{15}$ ceramic target was prepared as follows. The targets were sintered ceramics prepared by the solid state reaction of $BaCO_3$, $SrCO_3$, $NaCO_3$, and Nb_2O_5, and pressed into a cylinders of φ21.5 mm × 4 mm, then sintered again in air at 1350°C for 6 h. The density of BSNN target was approximately 98 %. The target was examined using X-ray diffraction (XRD), as shown in Fig. 2. The density of SBN ceramic target was approximately 94 %.

The PLD system was arranged in a symmetric configuration with a rotating substrate holder for compositional uniformity. The base pressure was ordinaly 2×10^{-8} Torr, and substrate was inserted from a load lock chamber to maintain a low base pressure. A KrF excimer laser (λ=248 nm) was used for ablation of target. The laser power density and repetition frequency were 200 mJ/cm^2 and 5 Hz, respectively. The film thickness was approximately 400 nm. The top Pt electrodes with a diameter of 0.2 mm were deposited on the film surface through a metal shadow mask by rf-magnetron sputtering. The as-deposited $Ba_2NaNb_5O_{15}$ thin films were annealed at 700°C in an O_2 atmosphere for 1h in order to investigate the effect of post-annealing.

The structural properties of the $Ba_{2-x}Sr_xNaNb_5O_{15}$ thin films were characterized by XRD. The surface morphologies were observed by AFM. The electrical properties were measured by using the ferroelectric property measurement system RT-6000HVS manufactured by Radiant Technologies. The polarization-voltage (*P-V*) hysteresis loops were measured using one-shot triangular waveforms with period of 50 ns.

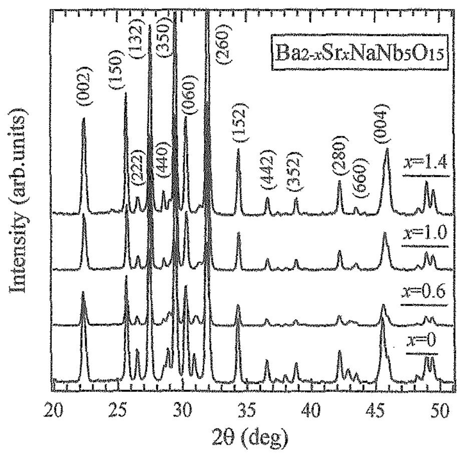

Fig. 2 XRD patterns as a function of Sr concentration in $Ba_{2-x}Sr_xNaNb_5O_{15}$ ceramics.

3. RESULTS AND DISCUSSION

Figure 3 shows the XRD patterns as a function of T_{sub} for the $Ba_{0.6}Sr_{1.4}NaNb_5O_{15}$ thin films. Po_2 was fixed at 7.5 mTorr. The (100) and (200) peaks of the LSTO substrates are observed at 2θ=22.8 ° and 46.5 °, respectively. The (002) and (004) peaks of the BNN thin films are observed at 2θ=22.4 ° and 45.7 °, respectively. The (350) peak is not observed in the thin film. The $Ba_2NaNb_5O_{15}$ thin films prepared at below T_{sub}=650°C do not show the (002) and (004) peaks, since the BNN thin films did not crystallize at below 650°C. The $Ba_{0.5}Sr_{0.5}NaNb_5O_{15}$ thin film at T_{sub}=700°C exhibits (002) and (004) peaks. Thus, the $Ba_{0.5}Sr_{0.5}NaNb_5O_{15}$ thin films prepared at 700 °C exhibit a strong *c*-axis orientation.

Figure 4 shows the XRD patterns as a function of Sr concentration in the $Ba_{2-x}Sr_xNaNb_5O_{15}$ thin films. Po_2 was fixed at 7.5 mTorr. The (002) and (004) peaks of these thin films are observed at near the substrate peaks. The existence of other phase is not observed in these thin films. The intensity of *c*-axis does not depend on Sr concentration. However, the (004) peak shifts to higher diffraction angle with Sr concentration, indicating the decrease of lattice constant. This result accords with the $Ba_{2-x}Sr_xNaNb_5O_{15}$ single crystals.

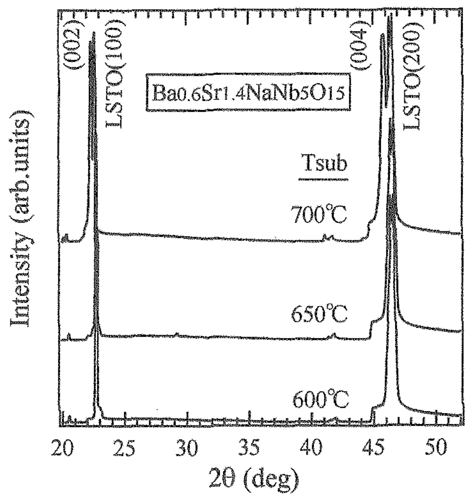

Fig. 3: XRD patterns as a function of T_{sub} in $Ba_{0.6}Sr_{1.4}NaNb_5O_{15}$ thin films. Po_2 is fixed at 7.5 mTorr.

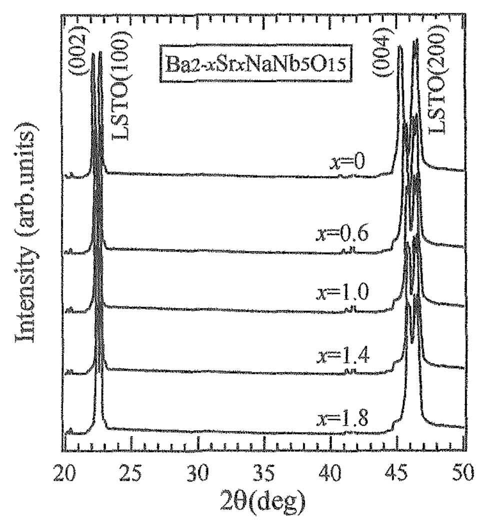

Fig. 4 XRD patterns as a function of Sr concentration in $Ba_{2-x}Sr_xNaNb_5O_{15}$ thin films.

Figure 5(a) shows the AFM image of $Ba_{0.6}Sr_{1.4}NaNb_5O_{15}$ thin film prepared on T_{sub}=700°C and Po_2=7.5 mTorr. The thin film consisted of small grains with diameter of ~50 nm. The surface roughness (R_{ms}) was approximately 11 nm against the film thickness of 400 nm.

Figure 5(b) shows the R_{ms} and grain size as a function of Sr concentration in $Ba_{2-x}Sr_xNaNb_5O_{15}$ thin films estimated from the AFM images. The $Ba_2NaNb_5O_{15}$ thin film consists of grains with diameter of ~80 nm and Rms of 7 nm. The grain size of $Ba_{2-x}Sr_xNaNb_5O_{15}$ ($x≠0$) is smaller than that of $Ba_2NaNb_5O_{15}$, although the R_{ms} does not depend much on Sr concentration. On the other hand, the authors have reported that the $Ba_2NaNb_5O_{15}$ thin film at Po_2>10mTorr and T_{sub}=700°C

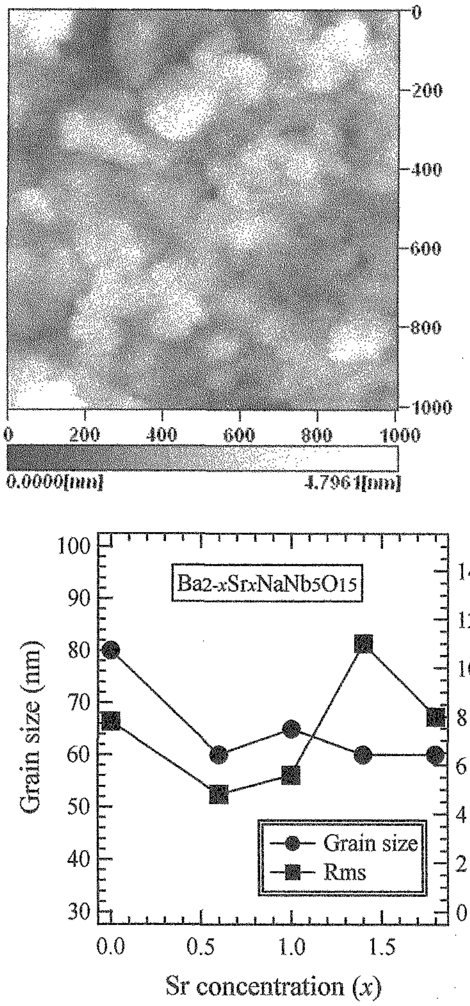

Fig. 5 (a) AFM image of $Ba_{0.6}Sr_{1.4}NaNb_5O_{15}$ thin films. (b) Surface roughness (R_{ms}) and grain size as a function of Sr concentration in $Ba_{2-x}Sr_xNaNb_5O_{15}$ thin films.

exhibits large R_{ms} and grain size. This originates from the three-dimensional islandlike crystal growth [7,9,10]. The particles ablated from the target migrate on the heated substrate and form crystal nuclei at step or kinds on the substrate due to the large energy at the interface of the BNN thin film and the substrate. In this study, $Ba_{2-x}Sr_xNaNb_5O_{15}$ thin films has prepared at Po_2=7.5 mTorr, which corresponds to the best condition of $Ba_2NaNb_5O_{15}$ thin film. Furthermore, the density of $Ba_{2-x}Sr_xNaNb_5O_{15}$ ($x \neq 0$) ceramics target is higher than that of $Ba_2NaNb_5O_{15}$ target. This may be the reason of small grain size for $Ba_{2-x}Sr_xNaNb_5O_{15}$ ($x \neq 0$) thin films.

Figure 6 shows the hysteresis loops as a function of Sr concentration in $Ba_{2-x}Sr_xNaNb_5O_{15}$ thin films. The as-deposited thin films did not exhibit ferroelectricity. We have already clarified that Na deficiency and oxygen vacancy are formed at the postannealing temperature above 750°C and the volatile of Na in $Ba_{2-x}Sr_xNaNb_5O_{15}$ thin film is controlled at the postannealing temperature below 750°C [7]. Therefore, these thin films were annealed at 700°C in oxygen atmosphere for 1 h in order to investigate the effect of postannealing. The postannealed $Ba_{2-x}Sr_xNaNb_5O_{15}$ thin film has controlled

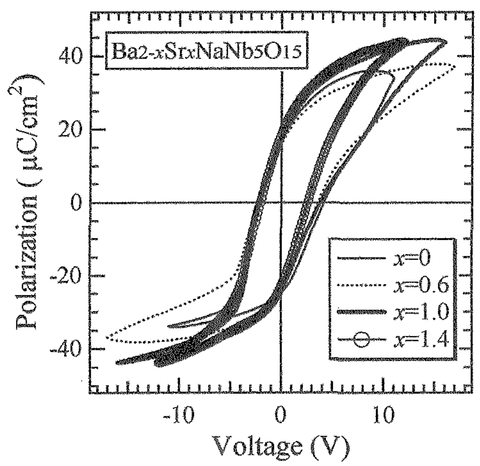

Fig. 6 *P-E* hysteresis loops as a function of Sr concentration in $Ba_{2-x}Sr_xNaNb_5O_{15}$ thin films.

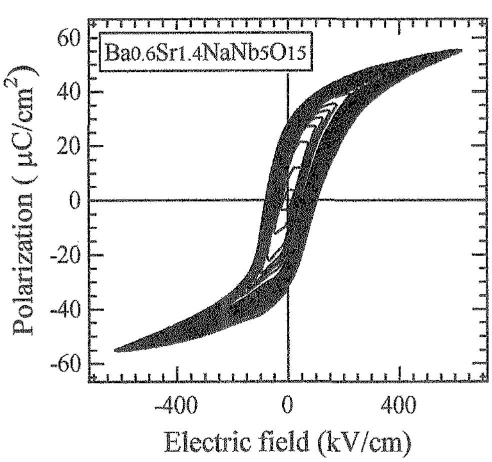

Fig. 7 *P-E* hysteresis loops as a function of voltage in $Ba_{0.6}Sr_{1.4}NaNb_5O_{15}$ thin film.

Na deficiency. The leakage current was improved from ~10^{-3} A/cm^2 to ~10^{-6} A/cm^2 by the postannealing. The obtained hysteresis loops exhibit nonsymmetrical shape. This might be originated to the conductivity of LSTO substrate. However, hysteresis loops seem to be improved by Sr substitution.

Figure 7 shows the hysteresis loops as a function of voltage in *c*-axis oriented $Ba_{0.6}Sr_{1.4}NaNb_5O_{15}$ thin film. The both $2P_r$ and $2E_c$ values increase rather steeply at a low applied voltage but do not change much beyond 20 V. The loop is nearly saturated at an applied voltage of 25 V. Then, the $2P_r$ and $2E_c$ were estimated to be 59.4 μC/cm^2 and 182 kV/cm, respectively. To further investigate the electrical properties of the $Ba_{2-x}Sr_xNaNb_5O_{15}$ thin films, it is necessary to perform a more systematic optimization of the deposition and the postannealing conditions of the $Ba_{2-x}Sr_xNaNb_5O_{15}$ thin films in the future study.

4. CONCLUSION

We have prepared the $Ba_{2-x}Sr_xNaNb_5O_{15}$ thin films on an LSTO substrates by PLD. The $Ba_{2-x}Sr_xNaNb_5O_{15}$ thin films crystallized at T_{sub}=700°C exhibit highly *c*-axis orientation. The lattice constant of *c*-axis decreases with increasing Sr concentration. The *c*-axis oriented $Ba_{2-x}Sr_xNaNb_5O_{15}$ thin films consist of small grain size and smooth surface. The postannealed $Ba_{2-x}Sr_xNaNb_5O_{15}$ thin films exhibit *P-E* hysteresis loops. The shape of hysteresis loop is improved by Sr substitution. When the Sr concentration is x=0.7, the $2P_r$ and $2E_c$ were estimated to be 59.4 μC/cm^2 and 182 kV/cm, respectively.

ACKNOWLEDGEMENT

We would like to thank Prof. S. Okamura for his useful discussion. This work was supported by a Grant-In-Aid for Scientific Research from the Ministry of Education, Culture, Sports, Science and Technology.

REFERENCES

[1] E. A. Giess, G. Berns, D. F. Okane and A. W. Smith: Appl. Phys. Lett. **11** (1967) 233.
[2] J. E. Geusic, H. J. Levinstein, S. Singh, R. G. Smith and L. G. Van Uitert: Appl. Phys. Lett. **12** (1968) 306.
[3] P. B. Jamieson, S. C. Abrahams and J. L. Bernstein: J. Chem. Phys. **48** (1968) 5048.
[4] S. H. Wemple and M. DiDomenico: J. Appl. Phys. **40** (1969) 735.
[5] M. Sogawa, T. Higuchi, T. Kamei and T. Tsukamoto: Jpn. J. Appl. Phys. **42** (2003) 6990.
[6] T. Higuchi, T. Kamei, M. Sogawa and T. Tsukamoto: Trans. Mater. Res. Soc. Jpn. **29** (2004) 1117.
[7] T. Kamei, T. Higuchi, M. Sogawa, Y. Ebina, T. Hattori and T. Tsukamoto: Jpn. J. Appl. Phys. **43** (2004) 6617.
[8] T. Higuchi, N. Machida, T. Yamasaki, T. Kamei, T. Hattori and T. Tsukamoto: Trans. Mater. Res. Soc. Jpn. **30** (2005) 23.
[9] L. G. van Uitert, J. J. Rubin, W. H. Grodkiewicz and W. A. Bonner: Mater. Res. Bull. **4** (1969) 63.
[10] M. Nakano, H. Tabata, K. Tanaka, Y. Katayama and T. Kawai: Jpn. J. Appl. Phys. **36** (1997) L 1331.

(Received December 10, 2005; Accepted January 31, 2006)